Electroporation Ablation of Liver Tumors: Numerical Strategies for Clinical Insights

On-line workshop, NYUAD 2024

Clair Poignard
Inria Research Center, Univ. Bordeaux, Team MONC

Experiments and applications of EP

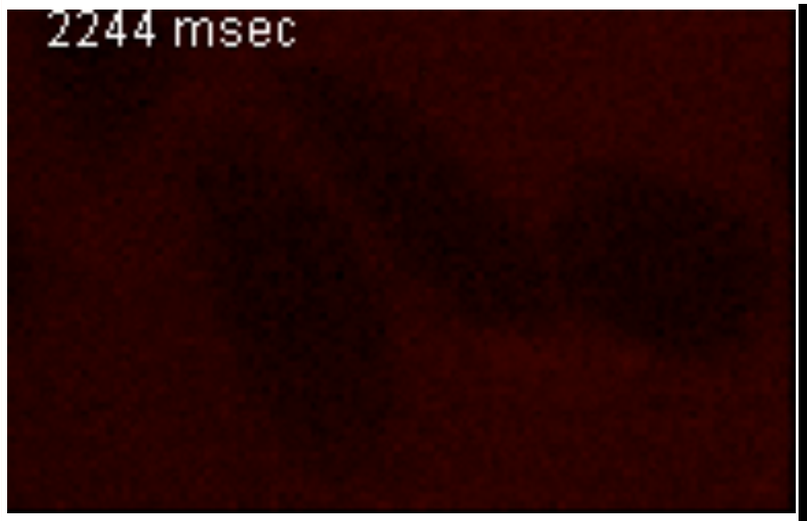

Postpulse PI uptake after EP pulse
From Escoffre et al. , BBA, 2011

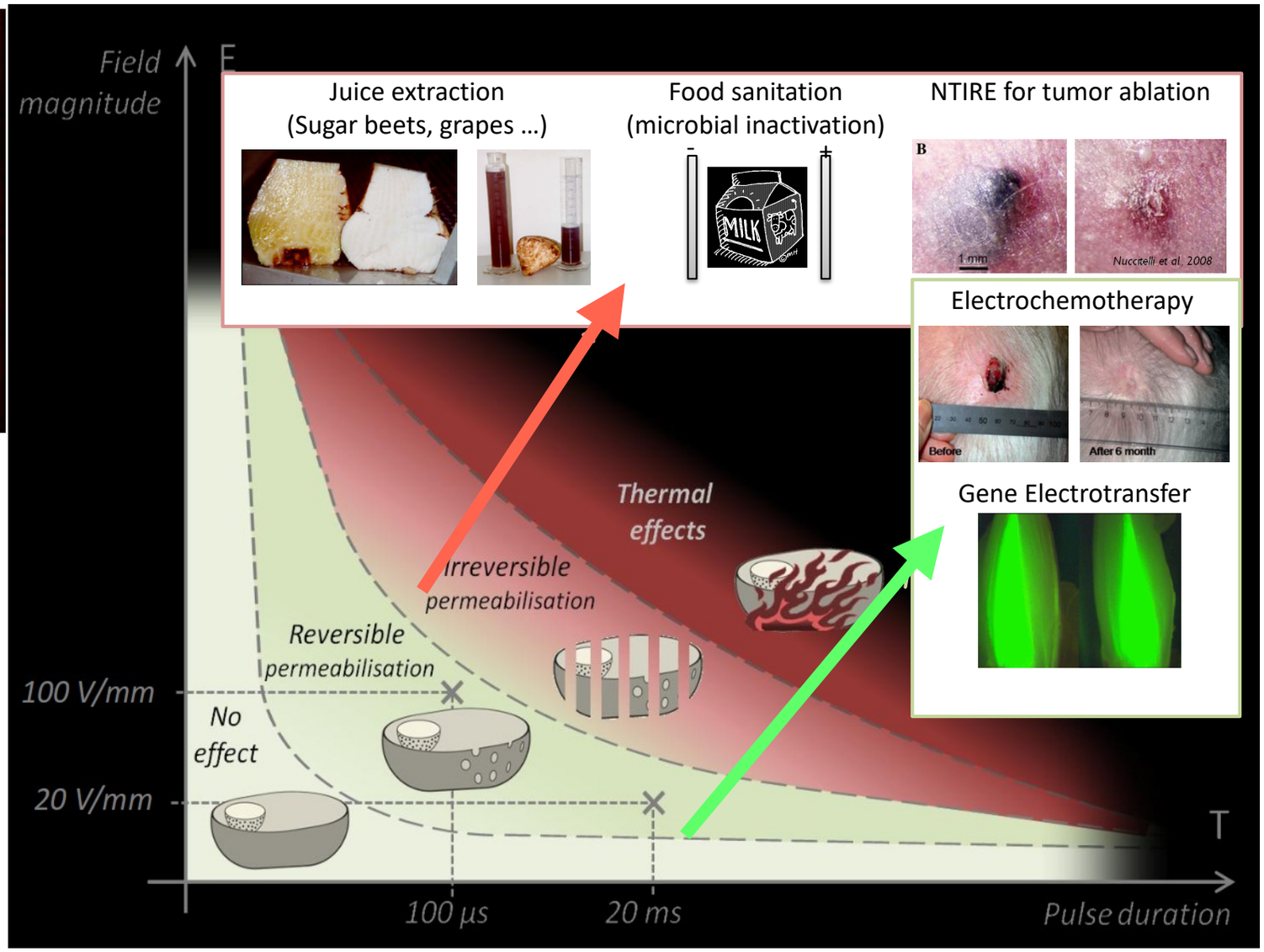

A.Silve

Heuristics of Cell EP

8pulses

$100\mu s, 400V/cm$

100pulses

$100\mu s, 1500V/cm$

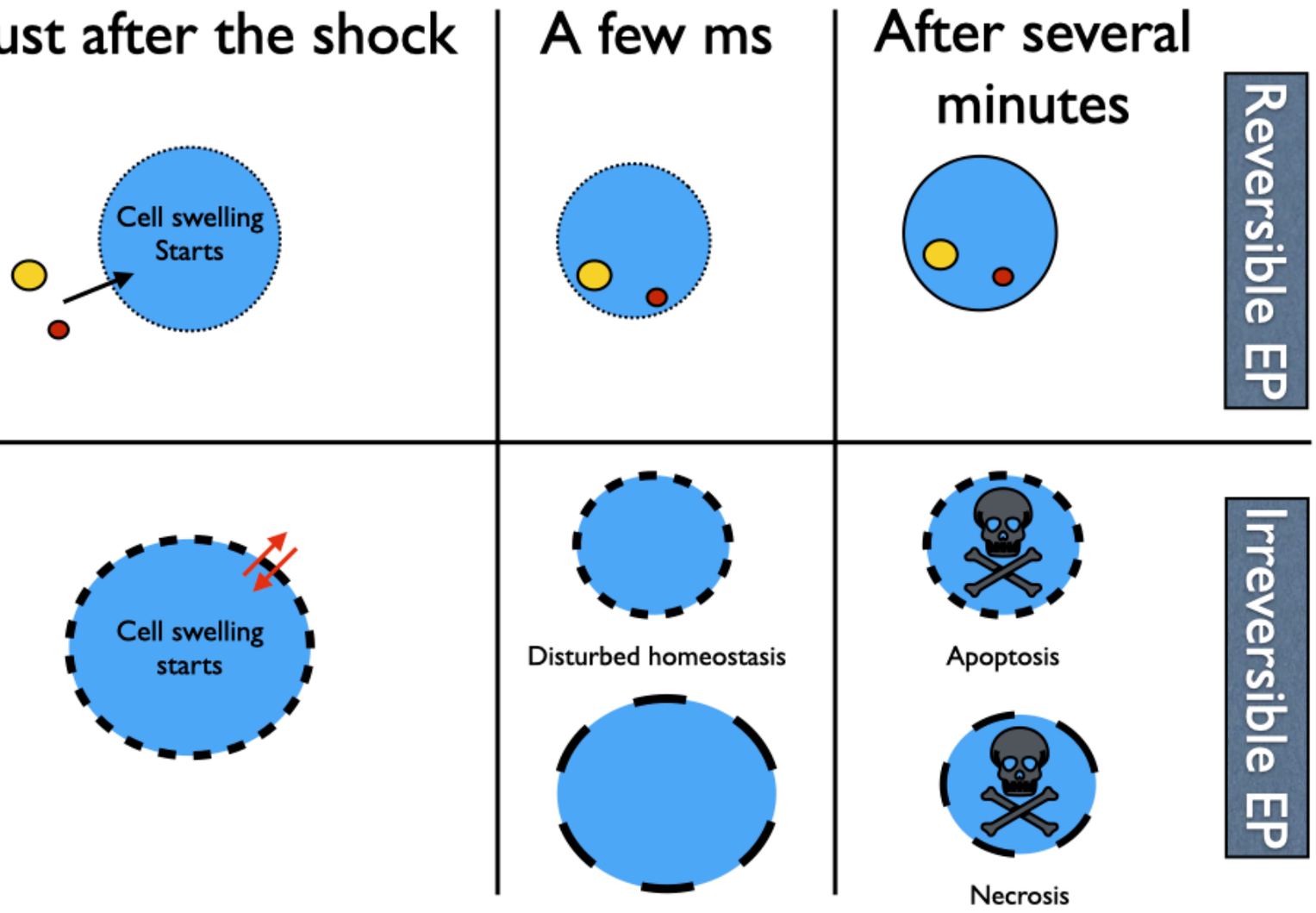

Not thermal death

01

Cell model of EP

Joint work with
A.Collin, P. Jaramillo-Aguayo,

Electroquasistatics in a cell

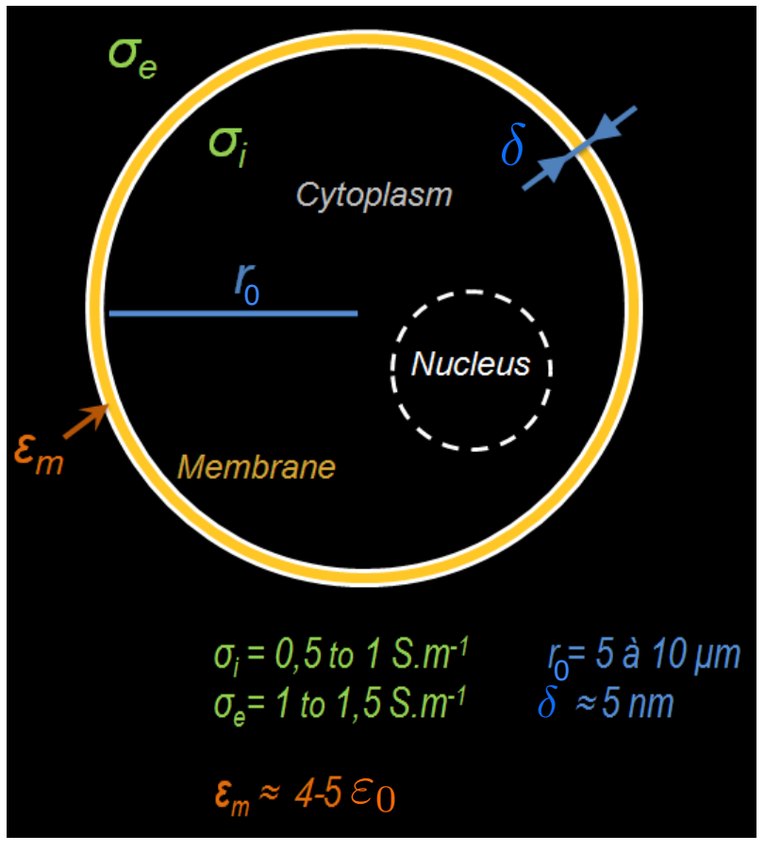

Electrical model of the cell

$$\partial_t \left(\nabla \cdot \left(\varepsilon \nabla u^\delta \right) \right) + \nabla \cdot \left(\sigma \nabla u^\delta \right) = 0$$

With the assumptions:

$$\varepsilon = \varepsilon_0 \begin{cases} \varepsilon_\mathrm{e} \\ \varepsilon_\mathrm{m} \\ \varepsilon_\mathrm{i} \end{cases} \sim \delta \begin{cases} C_\mathrm{e} \\ C_\mathrm{m} \\ C_\mathrm{i} \end{cases} \qquad \sigma = \begin{cases} \sigma_\mathrm{e} \\ \delta S_\mathrm{m} \\ \sigma_\mathrm{i} \end{cases}$$

Then the problem is approached by

$$\Delta u = 0, \quad \text{in } \mathcal{O}_\mathrm{c} \cup \mathcal{O}_\mathrm{e},$$
$$\sigma_\mathrm{e} \partial_n u|_{\Gamma+} = \sigma_\mathrm{c} \partial_n u|_{\Gamma-},$$
$$C_\mathrm{m} \partial_t [u]_\Gamma + S_\mathrm{m} [u]_\Gamma = \sigma_\mathrm{c} \partial_n u|_{\Gamma-},$$
$$u(t,\cdot)|_{\partial\Omega} = u_{imp}(t), \quad U(0,\cdot) = g.$$

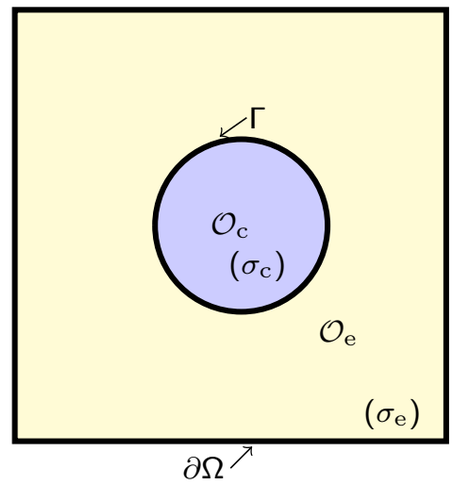

Dirichlet-to-Neumann maps

$$\Lambda_c : H^{1/2}(\Gamma) \to H^{-1/2}(\Gamma) \quad f \mapsto \vec{n_c} \cdot \sigma_c \nabla v_{c|_{\Gamma-}}$$, where v_c is the solution to $$\begin{cases} \nabla \cdot \sigma_c \nabla v_c = 0, \text{ in } \mathcal{O}_c, \\ v_{c|\Gamma} = f, \qquad v_{c|\partial\mathcal{O}_c \setminus \Gamma} = 0, \end{cases}$$

$$\Lambda_e : H^{1/2}(\Gamma) \to H^{-1/2}(\Gamma) \quad f \mapsto \vec{n_e} \cdot \sigma_e \nabla v_{e|_{\Gamma+}},$$ where v_e is the solution to $$\begin{cases} \nabla \cdot \sigma_e \nabla v_e = 0, \text{ in } \mathcal{O}_e, \\ v_{e|\Gamma} = f, \\ v_{e|\partial\mathcal{O}_e \setminus \Gamma} = 0, \end{cases}$$

$$\Lambda_o : H^{1/2}(\partial\Omega) \to H^{-1/2}(\Gamma) \quad g \mapsto \vec{n_e} \cdot \sigma_e \nabla v_{|_{\Gamma+}}$$, where v_b is the solution to $$\begin{cases} \nabla \cdot \sigma_e \nabla v_b = 0, \text{ in } \mathcal{O}_e, \\ v_{|\Gamma} = 0, \\ v_{|\partial\Omega} = g. \end{cases}$$

Formulation on the membrane

Thanks to the 3 DtN maps, one defines

$$\mathcal{L}_\Gamma = \Lambda_c \left(\mathrm{Id} + \Lambda_e^{-1}\Lambda_c\right)^{-1}, \quad \mathcal{L}_0 = \Lambda_c \left(\mathrm{Id} + \Lambda_e^{-1}\Lambda_c\right)^{-1} \Lambda_e^{-1}\Lambda_0$$

Then the transmembrane voltage satisfies

$$C_\mathrm{m}\partial_t v_\mathrm{m} + \left(S_\mathrm{m} + \mathcal{L}_\Gamma\right) v_\mathrm{m} = \mathcal{L}_0 g$$

Note the operator $\mathcal{L}_\Gamma$ is m-accretive with dense domain in $H^1(\Gamma)$ (Kavian, Leguèbe, CP, Weynans, JMB 2014)

In a spherical cell of radius r_c in a unidirectional uniform EF *E*

$$\boxed{C_\mathrm{m}\partial_t v + \left(S_\mathrm{m} + \frac{1}{r_c}\frac{2\sigma_e\sigma_c}{2\sigma_e+\sigma_c}\right) v = \frac{3\sigma_e\sigma_c}{2\sigma_e+\sigma_c} E\cos\varphi}$$

Charging time: $\tau_m = \dfrac{2\sigma_e+\sigma_c}{2\sigma_e\sigma_c} \dfrac{r_c C_m}{1+\frac{2\sigma_e+\sigma_c}{2\sigma_e\sigma_c} r_c S_m} \sim 0.1\mu s$

Free-energy of the membrane

$$\mathcal{E}(\phi, V_m) = \frac{\kappa}{2} \int_\Gamma |\nabla \phi|^2 \, ds + \int_\Gamma W_m(\phi) \, ds - \frac{1}{2} \int_\Gamma C_m(\phi) V_m^2 \, ds.$$

$$W_m(\phi) := 16 a_1 \phi^2 (1-\phi)^2 + 8 a_2 (\phi + 1/2)(\phi - 1)^2$$

$$C_m(\phi) = C_{lipid}\, \phi + C_{water}(1-\phi)$$

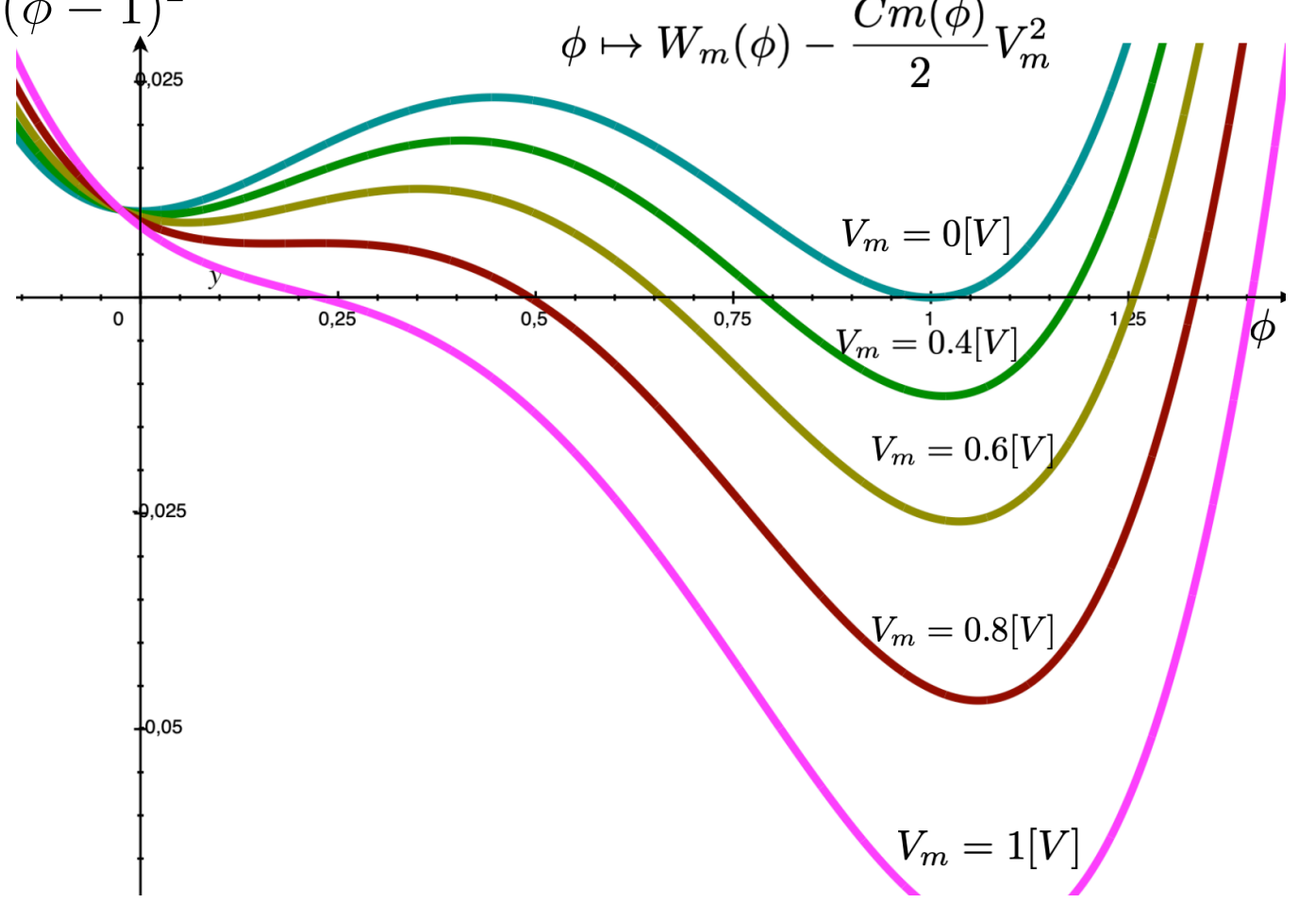

The coupling the PDEs

$$C_m(\phi)\partial_t V_m + \left(S_m(\phi) + \mathcal{L}_\Gamma\right) V_m = \mathcal{L}_0 g$$

$$\partial_t \phi - D_0 \Delta \phi = \alpha W_m'(\phi) + \frac{\alpha}{2} C_m'(\phi) V_m^2,$$

$$\phi(0,\cdot) = \phi_0(\cdot), \;\; V_m|_{t=0} = V_m^0$$

$$S_m(\psi) = \frac{\sigma_m(\psi)}{h}, \quad \text{where}$$

$$\sigma_m(\psi) = \frac{1 + \tanh(k_0(\psi - \phi_{\text{th}}))}{2}(\sigma_w - \sigma_l) + \sigma_l,$$

Property [Jaramillo, Collin, CP. JoMB2023]

- Transition interface of order $\mathcal{O}(\sqrt{\frac{D_0}{64\alpha a_1}}) \sim 1nm$
- Time for pore creation of order $t_0 = \mathcal{O}(\frac{1}{64\alpha a_1} \log\left(\frac{D_0}{64\alpha a_1 L^2}\right)) \sim 1ns$
- After the pulse, the pore shape is driven by mean- curvature

Instabilities for spherical or flat membranes

For spherical and flat membranes the operators are diagonalisable in the same basis and we have the following sufficient condition to get instabilities:

$$C_m''(\phi) > c(\phi^2 + (6 - \frac{3a_2}{2a_1}\phi + (1 - \frac{3a_2}{4a_1} + \frac{D_0}{64a_1}\lambda_n)$$

Linear model of capacitance are stable for the Allen-Cahn model.

The model of C_m comes from Looyenga [20]

$$C_m : \quad \psi \mapsto \frac{\epsilon_0}{h}\left(\left[\epsilon_l^{1/3} + \psi(\epsilon_w^{1/3} - \epsilon_l^{1/3})\right]^3 \vartheta_1(\psi) + \epsilon_w \vartheta_2(\psi)\vartheta_3(\psi)\right),$$

where

$$\vartheta_i(\psi) = \frac{1 + \tanh(k_i(\psi - \phi_i^{\text{th}}))}{2}, \qquad i = 1, 2, 3,$$

Numerical scheme based on FFT

$$\begin{cases} \Phi^* = e^{\delta t \triangle} \Phi^n, \\ \frac{V^* - V^n}{\delta t} + \frac{1}{2}\left(\frac{1}{C_m(\Phi^*)}(\Lambda - \lambda_{\vec{0}})V^* + \frac{1}{C_m(\Phi^n)}(\Lambda - \lambda_{\vec{0}})V^n\right) = \frac{1}{2}\left(\frac{G^n}{C_m(\Phi^n)} + \frac{G^{n+1}}{C_m(\Phi^*)}\right) \end{cases}$$

$$\begin{cases} \begin{bmatrix} \Phi^{n+1} \\ V^{n+1} \end{bmatrix} = \begin{bmatrix} \Phi^* \\ V^* \end{bmatrix} + \delta t F\left(\begin{bmatrix} \Phi^* \\ V^* \end{bmatrix}\right) + \frac{\delta t^2}{2} \mathbb{J}F_{|(\Phi^*, V^*)} \cdot F\left(\begin{bmatrix} \Phi^* \\ V^* \end{bmatrix}\right) \end{cases}$$

where

$$F : \begin{bmatrix} \phi \\ v \end{bmatrix} \mapsto \begin{bmatrix} -\alpha \mathcal{W}'(\phi) + \frac{\alpha}{2} C_m'(\phi) v^2 \\ -\frac{(S_m(\phi) + \lambda_{\vec{0}})}{C_m(\phi)} v \end{bmatrix}$$

Main idea: symmetrize the problem

$$\left[Id + \frac{\delta t/2}{\sqrt{C_m(\Phi^*)}}(\Lambda - \lambda_{\vec{0}})\frac{1}{\sqrt{C_m(\Phi^*)}}\right] Y = \sqrt{C_m(\Phi^*)}\left[\left[Id - \frac{\delta t/2}{C_m(\Phi^n)}(\Lambda - \lambda_{\vec{0}})\right] V^n + \frac{\delta t}{2}\left[\frac{G^n}{C_m(\Phi^n)} + \frac{G^{n+1}}{C_m(\Phi^*)}\right]\right]$$

Water content of the membrane

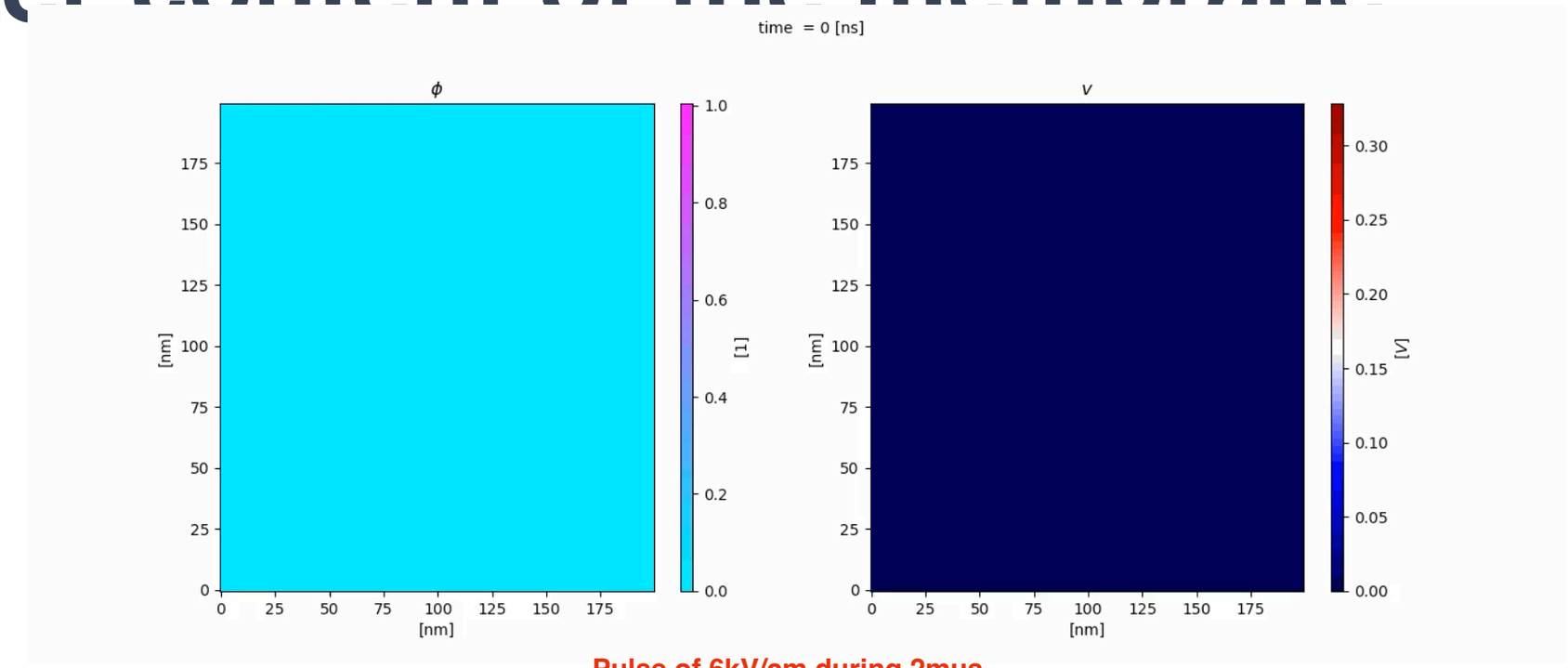

Pulse of 6kV/cm during 2mus

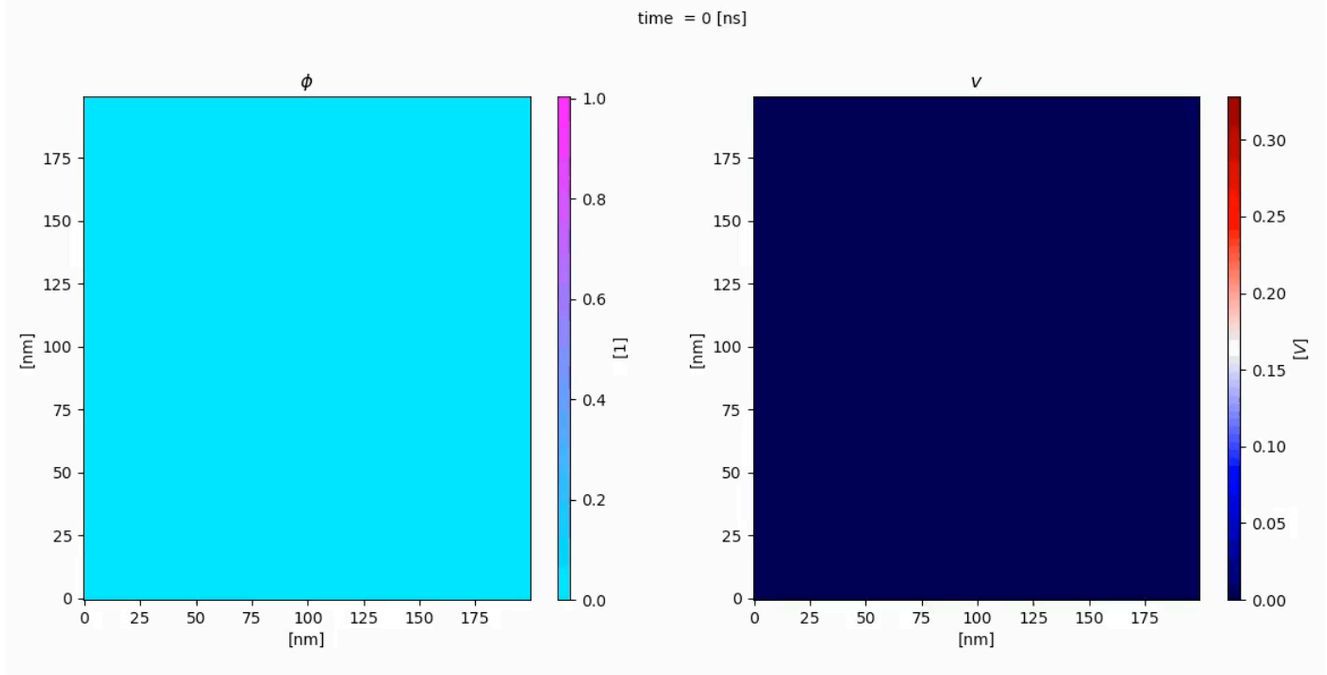

Pulse of 6kV/cm during 4mus

02

Liver ablation by EP

Joint work with

B. Denis de Senneville, L. Lafitte, D. Voyer

O. Sutter, O. Séror, JP Tasu

A centripetal energy deposit

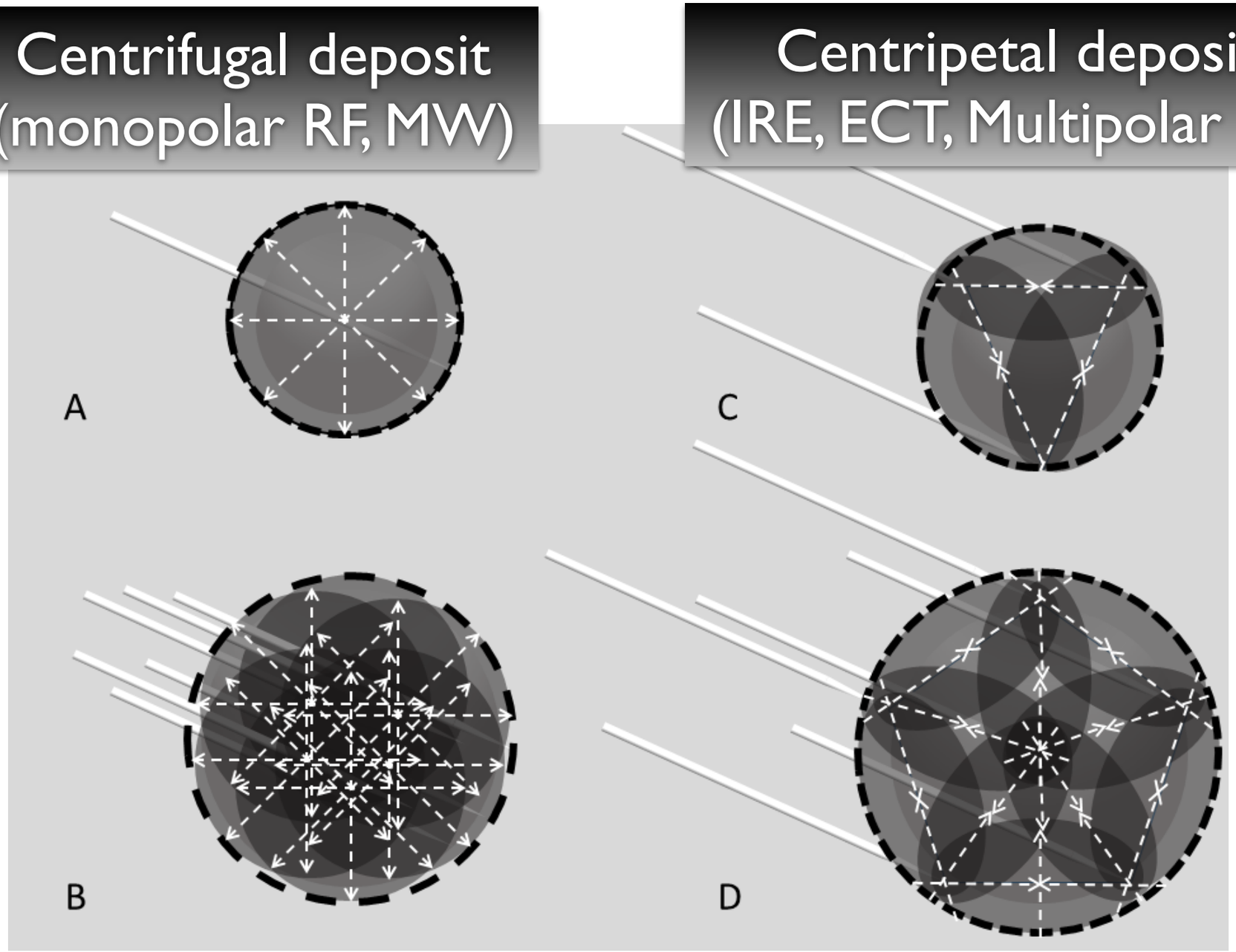

Hepatocellular carcinoma (HCC)

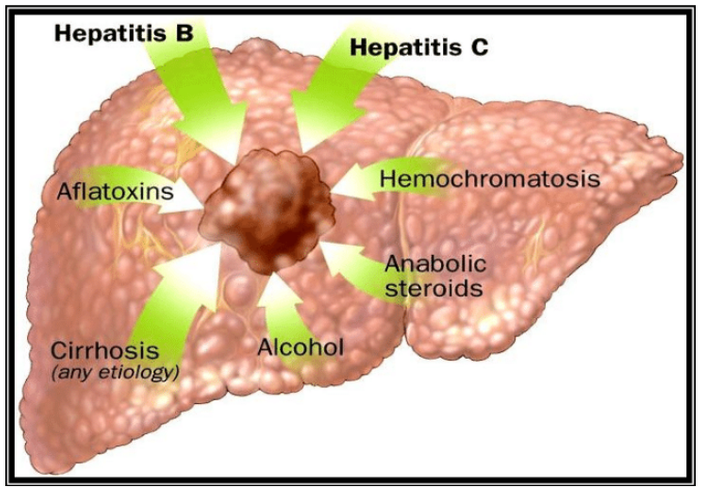

Causes of liver cancer (hepatocellular carcinoma)
Credit: Johns Hopkins Kimmel Cancer Center

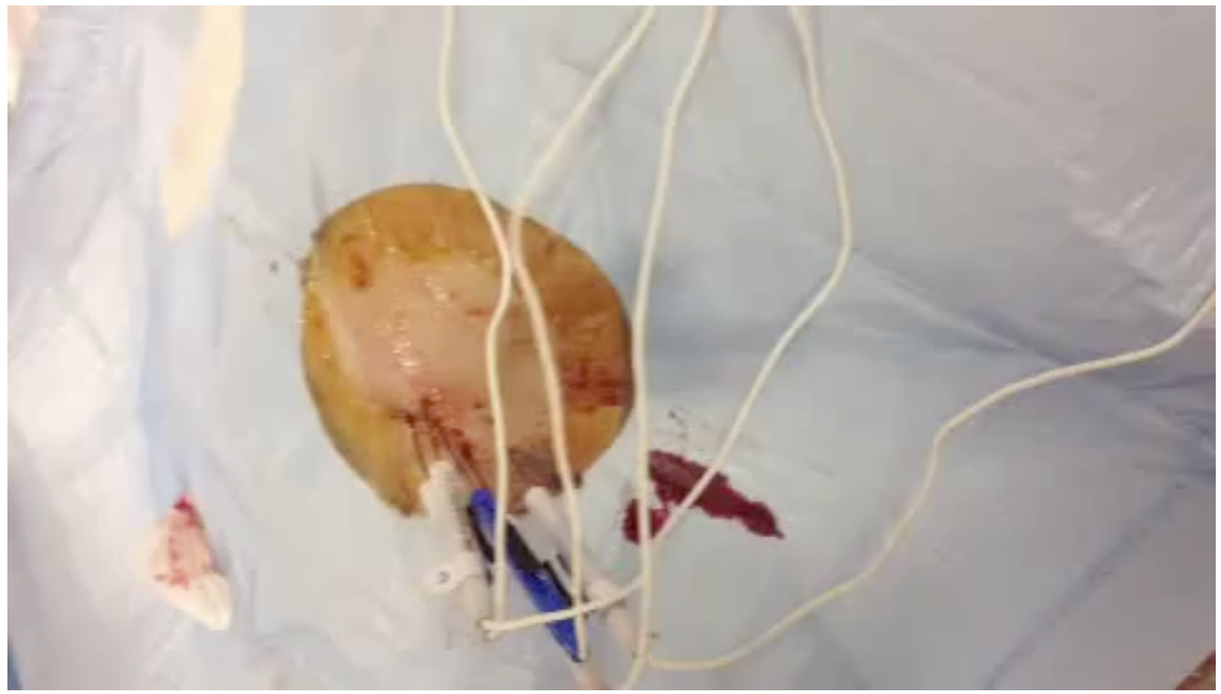

- No surgery for advanced disease. No chemotherapy. Only TKI with a poor efficacy (~+3mo of OS).
- Percutaneous ablation (especially RF ablation) is used for nodules limited in number (<3) and diameter (3cm) but RFA is however prohibited for some tumors near vital structures.

Irreversible EP is a promising alternative since it is minimally thermal.

Heuristics of liver tumor ablation by EP

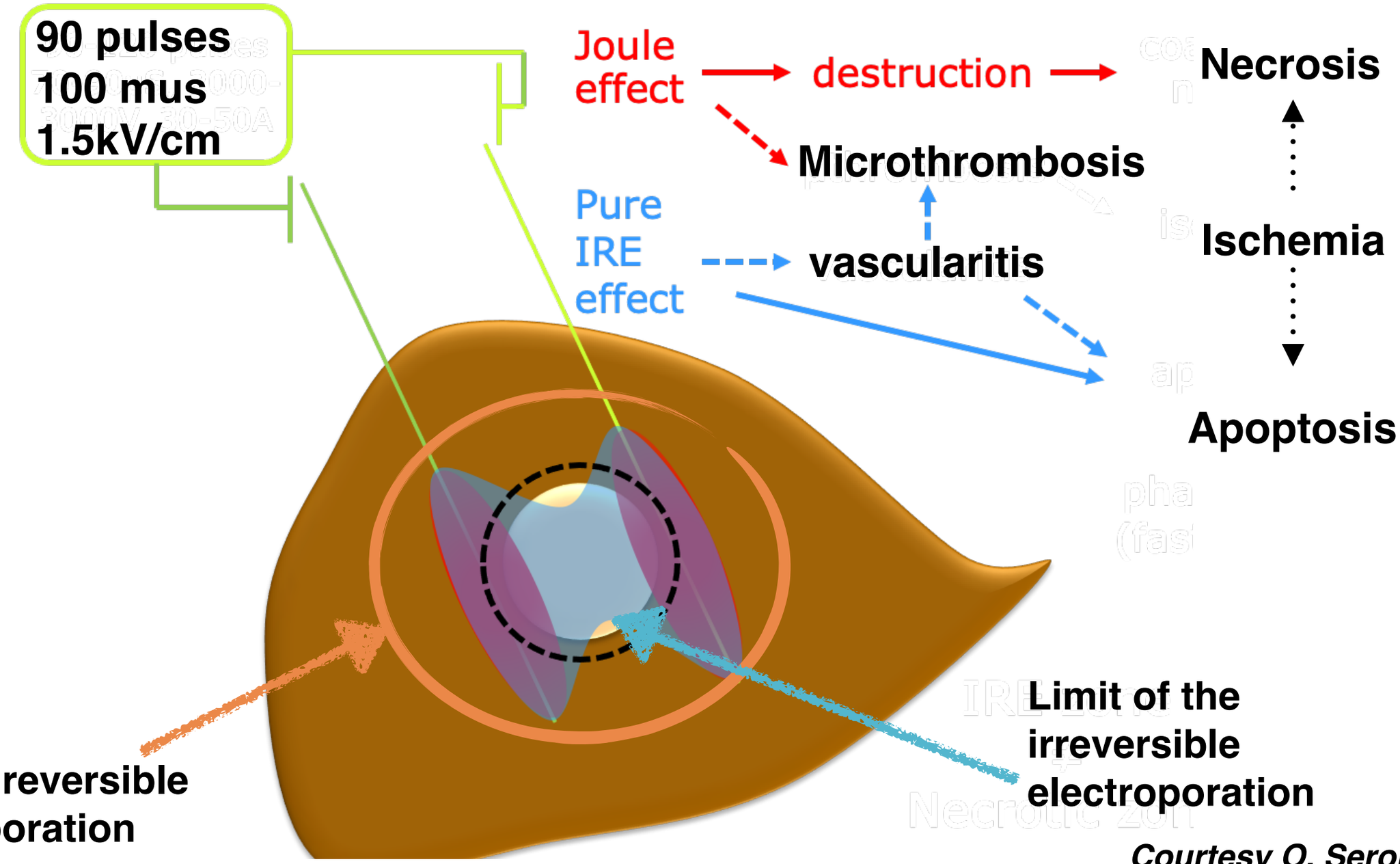

Courtesy O. Seror

Static tissue model of EP

$$-\nabla \cdot (\Sigma_{eq}(|\nabla\phi|)\nabla\phi) = 0,$$

$$\phi|_{\mathcal{E}^\pm} = g^\pm$$

$$\text{where} \quad \Sigma_{eq}(|\nabla\phi|) = |\Omega_e|\sigma_e + \frac{|\Omega_c|\sigma_c}{1 + \frac{|\Omega_c|}{|\Gamma_m|}\frac{\sigma_c}{S_m(|\nabla\phi|)}},$$

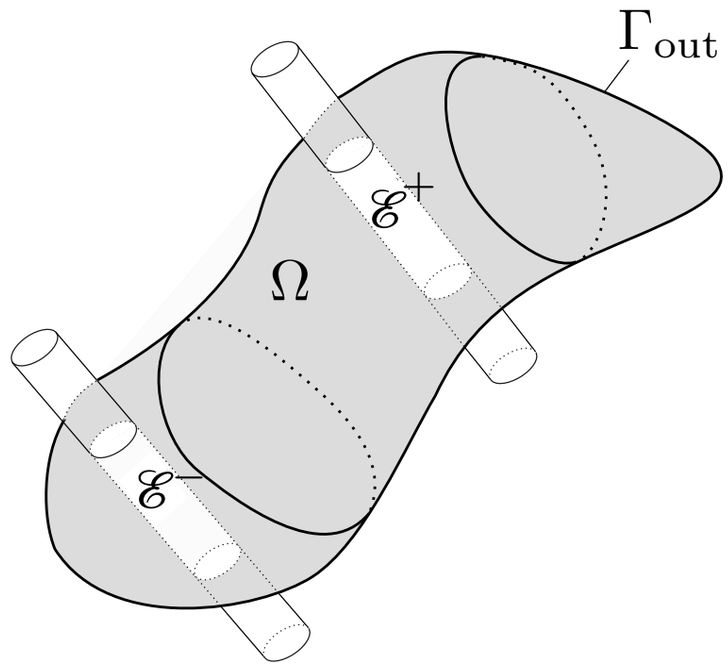

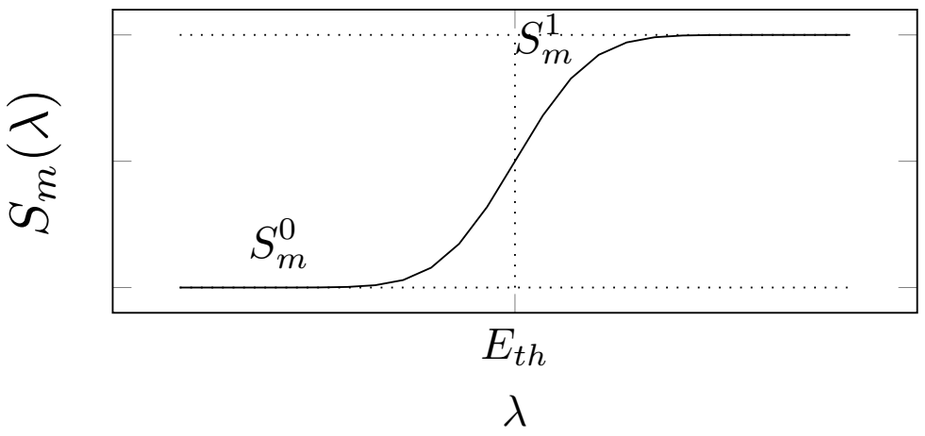

The problem is equivalent to minimise

$$J(\phi) = \int_\Omega \int_0^{|\nabla\phi|} s\Sigma_{eq}(s)dsdx - \int_\Omega f\phi dx$$

which is strictly convex on $H^1(\Omega)$

For a comparison of existing EP models see:

G. Jankowiak et al. Comparison and calibration of different electroporation models. Application to rabbit livers experiments. ESAIM: Proceedings and Surveys, 67, 242-260. 2020.

IRE in real life: very tricky procedure!

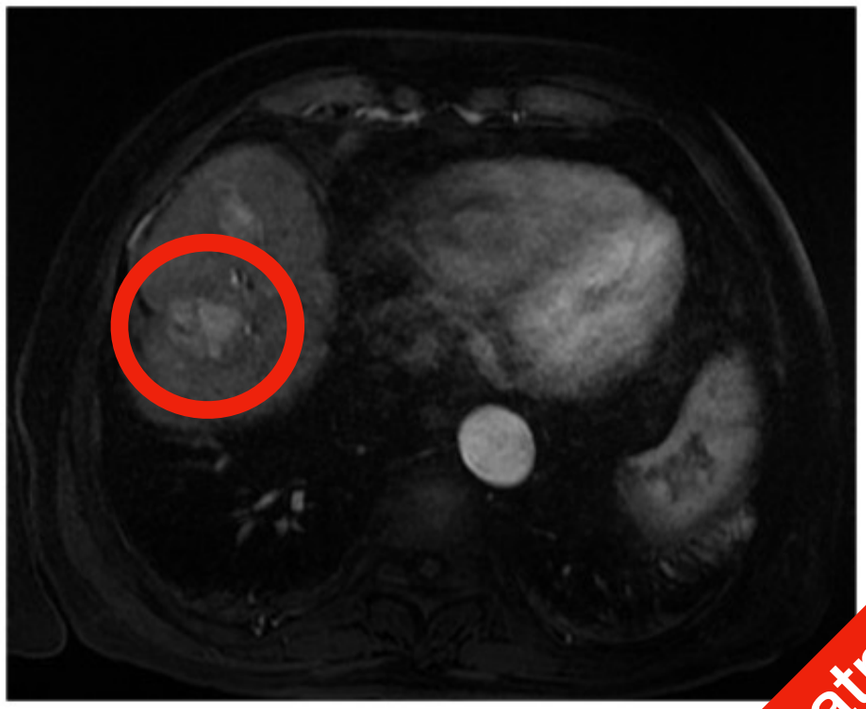

Pretreatment image

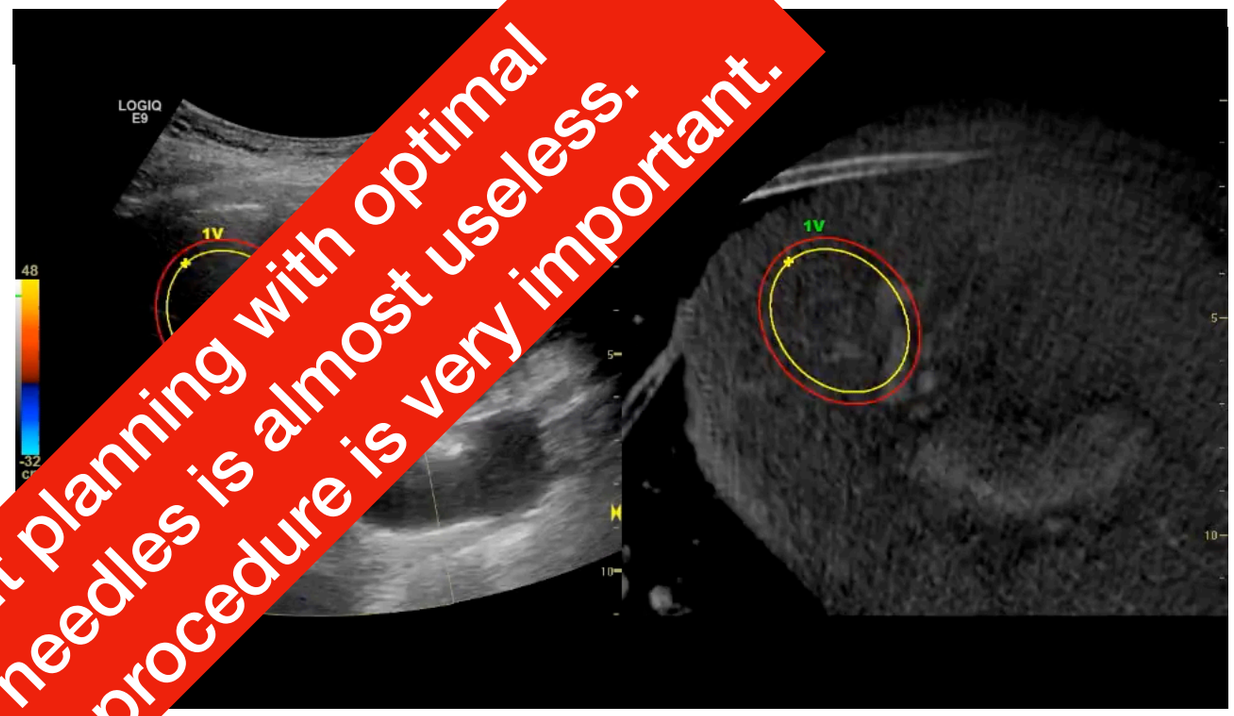

Needle positionning using fusion imaging

Validation

Numerical treatment planning with optimal placement of the needles is almost useless. A feedback on the procedure is very important.

Numerical workflow

	Preoperative Session (Step 1)	Interventional session (Step 2)	
Clinical Workflow	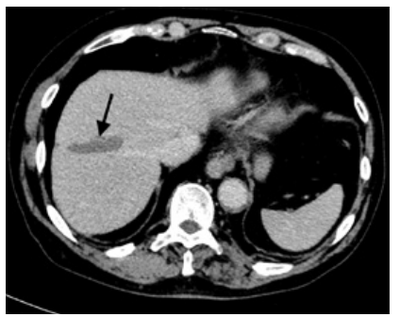 CT-scan (Day -30)	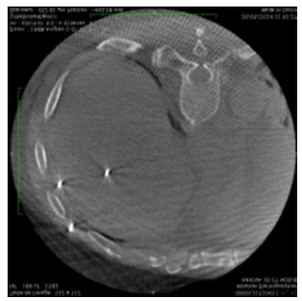 CBCT after needle insertion	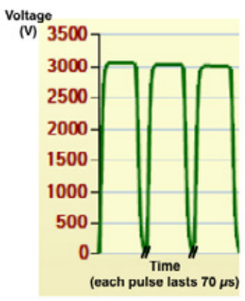 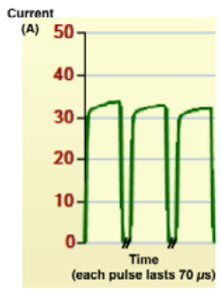 Voltage and Current chrono-grams recorded by Nanoknife
Numerical Processes	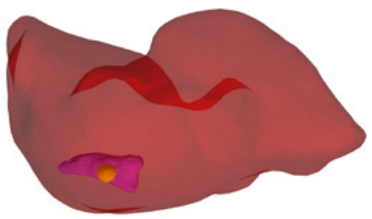 ROIs Extraction	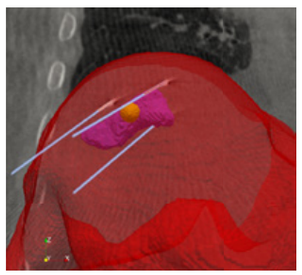 ROIs registration on the CBCT	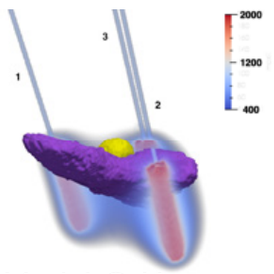 Model Calibration and Simulation

Gallinato, Denis de Senneville, Séror,C.P, PMB 2019

université de BORDEAUX

Inria

Non rigid multimodal image registration

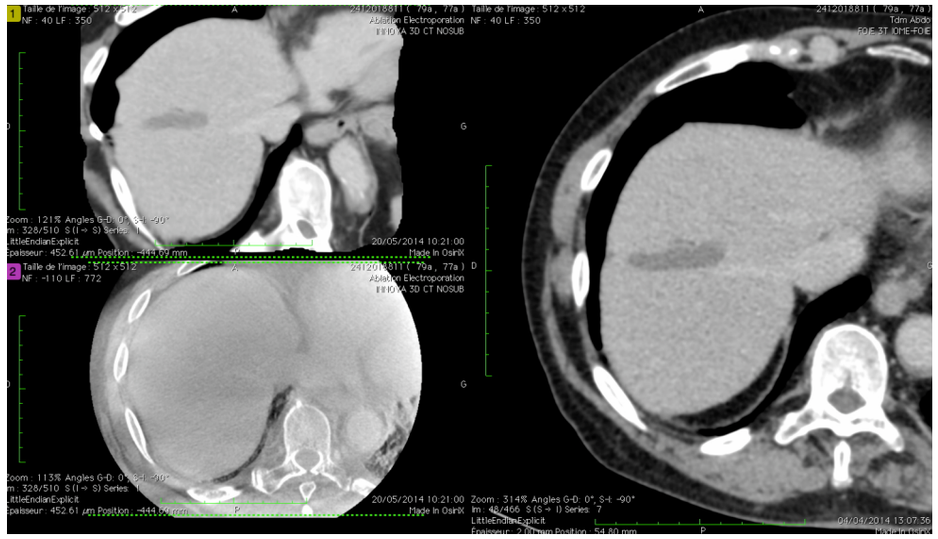

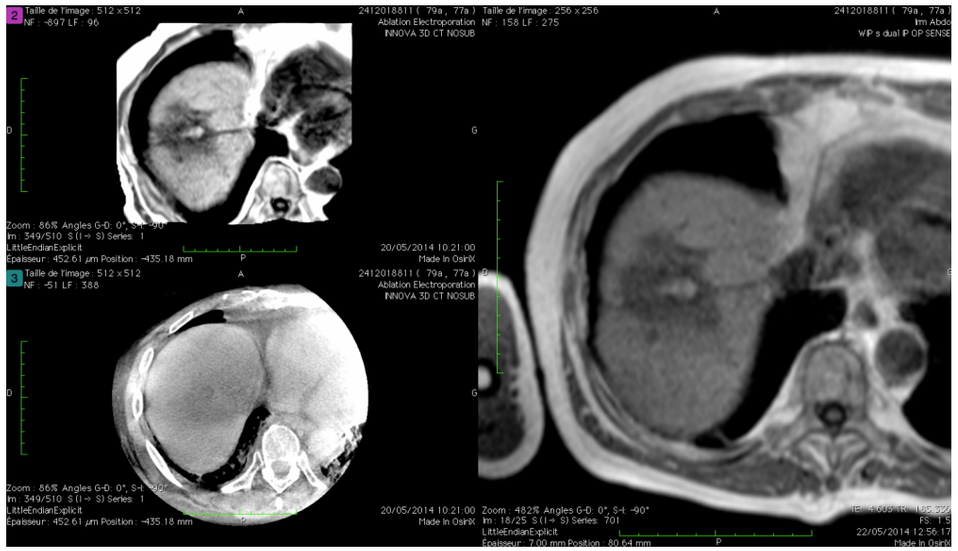

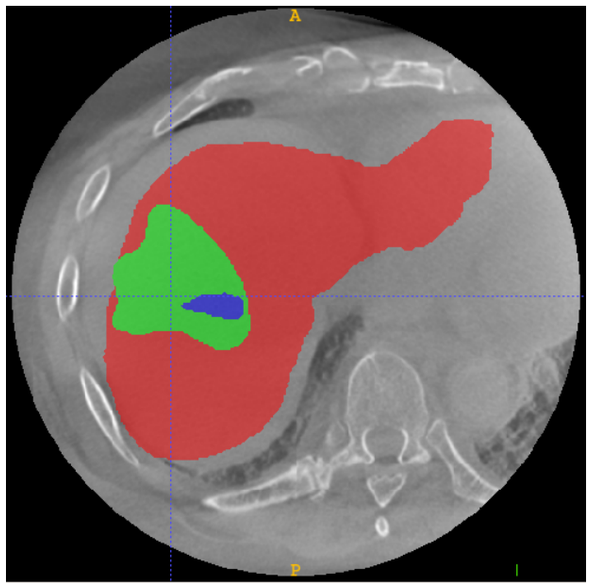

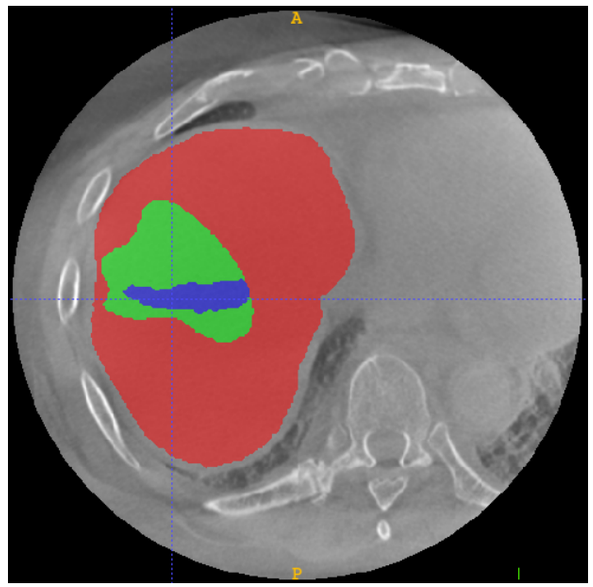

Comparison rigid/nonrigid registration

$$C(T) = \frac{\int_\Gamma \left| \vec{\nabla}_I(T(\vec{r})) \cdot \vec{\nabla}_J(\vec{r}) \right| \mathrm{d}\vec{r}}{\int_\Gamma \|\vec{\nabla}_I(T(\vec{r}))\|_2 \, \|\vec{\nabla}_J(\vec{r})\|_2 \, \mathrm{d}\vec{r}} \qquad D(T) = \mathrm{e}^{-C(T)}$$

Minimization of E, (De Senneville et al 2016))

$$E(T) = \int_\Omega D(T) + \frac{\alpha}{2}(\|\vec{\nabla}u\|_2^2 + \|\vec{\nabla}v\|_2^2 + \|\vec{\nabla}w\|_2^2)\mathrm{d}\vec{r}$$

université de BORDEAUX

Inria

Recovering the local conductivity

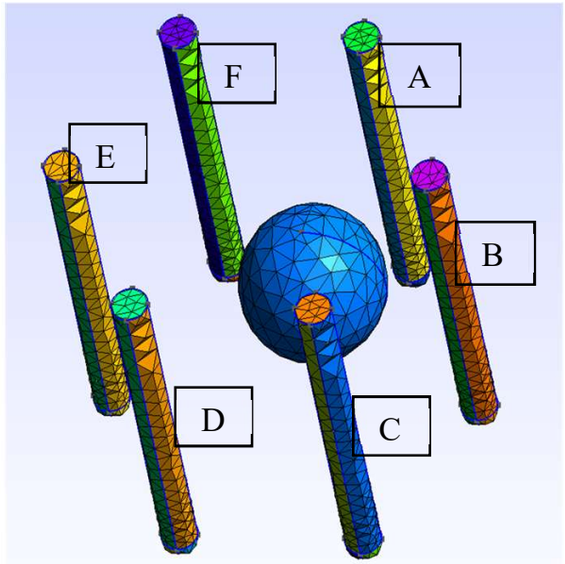

$$\text{Problem } m \begin{cases} \nabla . (\sigma \nabla \phi_m) = 0 \ \ in \ \ \Omega \\ \phi_m|_{\Gamma_{m+}} = +V \\ \phi_m|_{\Gamma_{m\_}} = -V \\ \phi_m|_{\Gamma_p} = V_p \ \ with \iint_{\Gamma_p} \sigma \frac{\partial \phi_m}{\partial n} d\Gamma = 0 \\ p = \{1, 2, \cdots, 6\} \setminus \{m_+, m_-\} \\ \sigma \frac{\partial \phi_m}{\partial n} = 0 \ \ on \ \ \partial\Omega \setminus \{\Gamma_1, \cdots, \Gamma_6\} \end{cases}$$

$$I_m = \iint_{\Gamma_{m+}} \sigma \frac{\partial \phi_m}{\partial n} d\Gamma = \frac{1}{2V} \iiint_{\Omega} \sigma \, |\nabla \phi_m|^2 \ d\Omega$$

$$\boxed{Z_{ij} = \frac{1}{I_i \, I_j} \iiint_{\Omega} \sigma \, \nabla \phi_i \, \nabla \phi_j \, d\Omega}$$

Main idea: Minimize measured and numerical impedance.
Tools: combine Medical Imaging and standard EIT assuming piecewise constant conductivities to stabilize the inverse problem

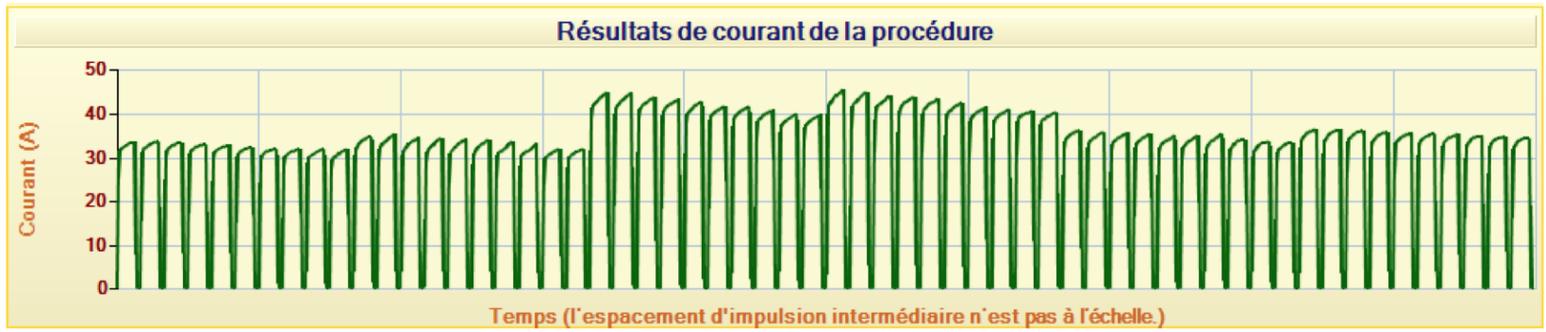

ClinicalIRE: a software dedicated to dose map computing

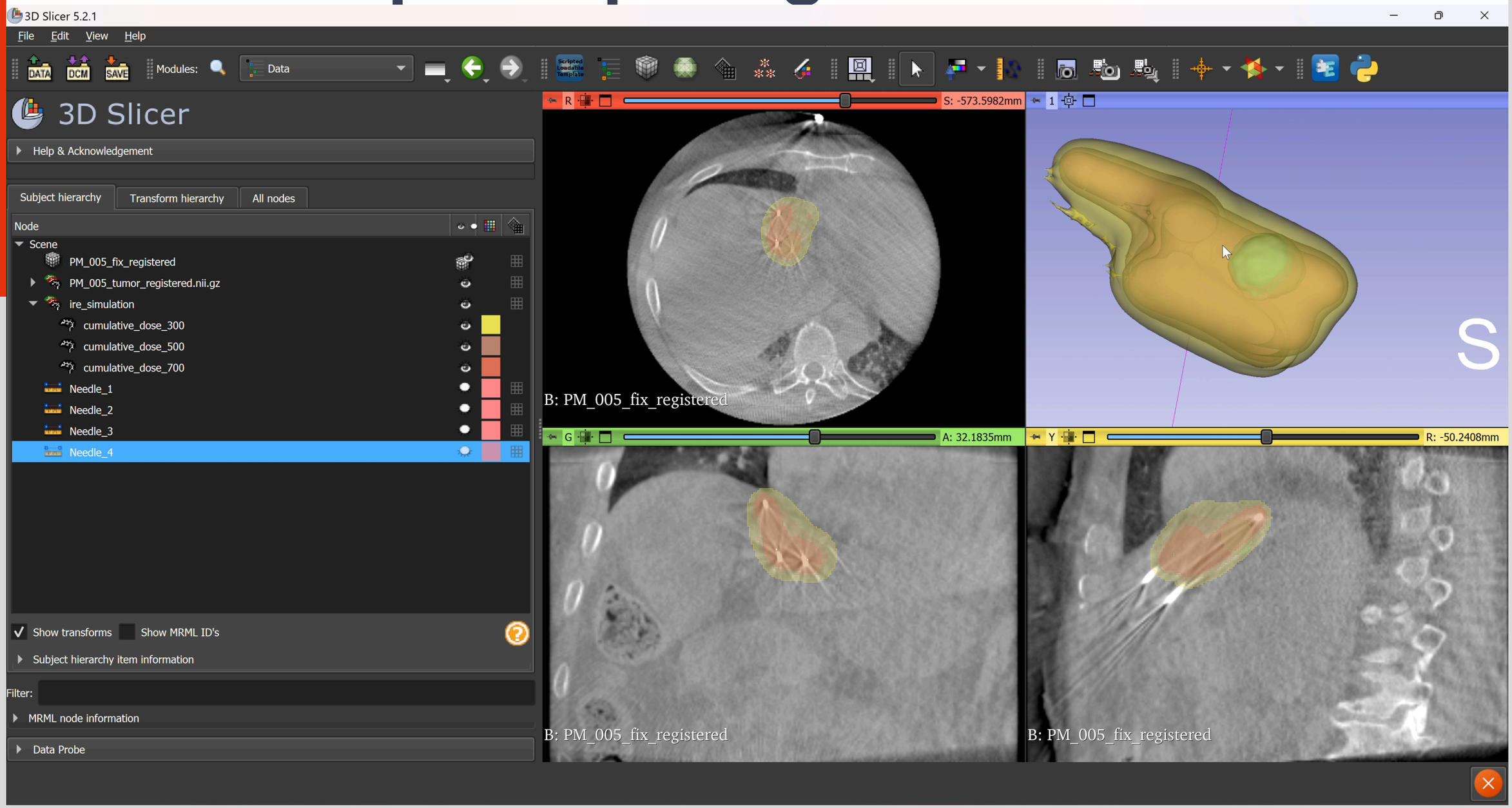

Coverage of the tumour by EF

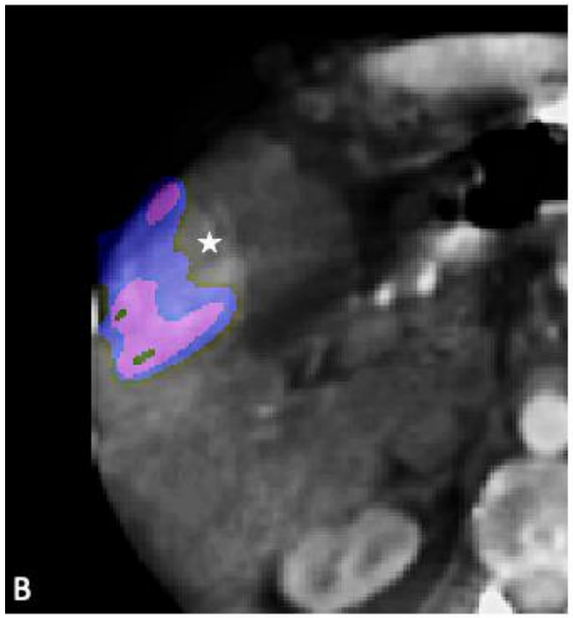

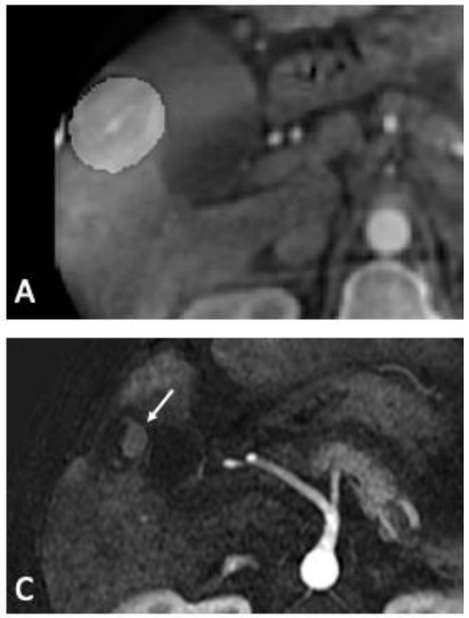

Typical profile of treatment failure.
The tumor is only partially covered by the EF

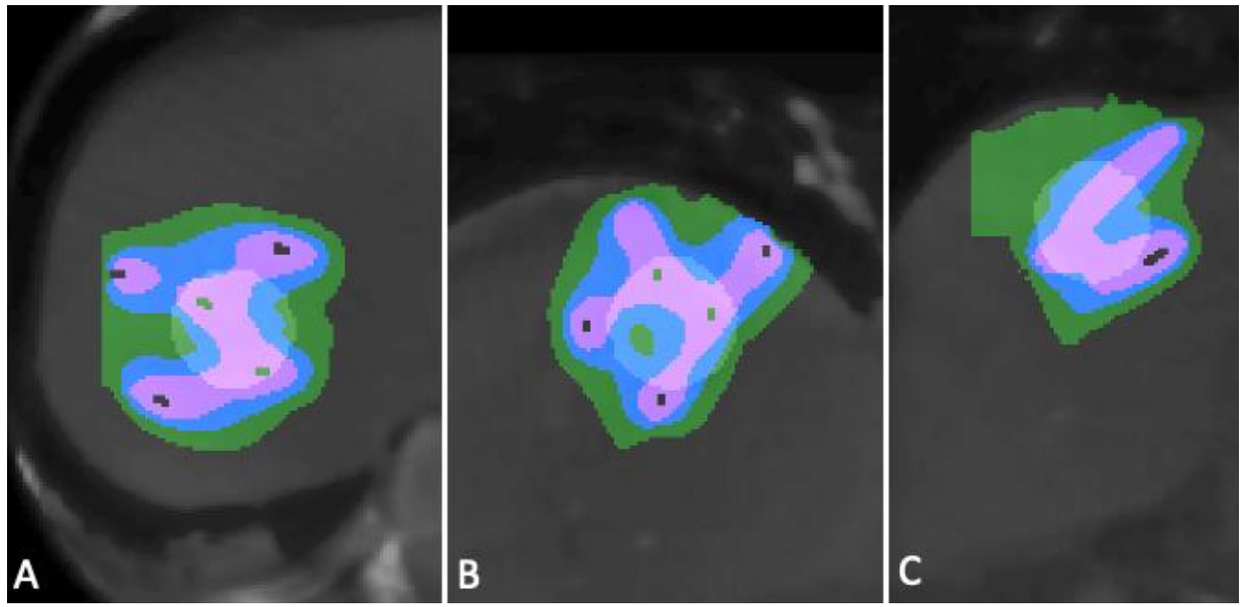

Typical profile of treatment success.
The tumor is well covered by the EF

The software PrimetimeIRE is in the test phase in the operating room of Avicenne hospital.

Comparing with clinical follow-up

Retrospective study with patient follow-up

Patient number	RECIST (mm)	% coverage 350V/m	% coverage 700V/m	Follow-up
P4	27	100	90	Transplanted
P14_1	21	100	85	Relapse at 18mo
P14_2	18	60	40	
P18	22	40	10	New IRE at 27mo
P24	43	90	75	No relapse at 51mo
P26	12	100	80	No relapse at 28mo
P28	18	100	75	No relapse at 5mo
P29	50	100	85	Transplanted
P30	31	55	30	Rapid disease prog.
P32	30	35	15	New IRE at 18mo
P37	34	90	60	No relapse at 4mo
P43	38	75	55	Relapse at 7mo

Master thesis of O. Sutter, MD

New interpretations of MRI at D+3

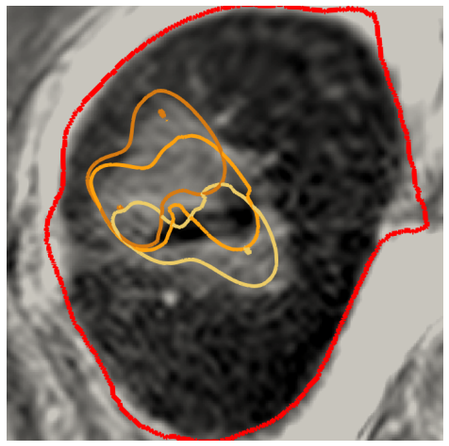

T2 w

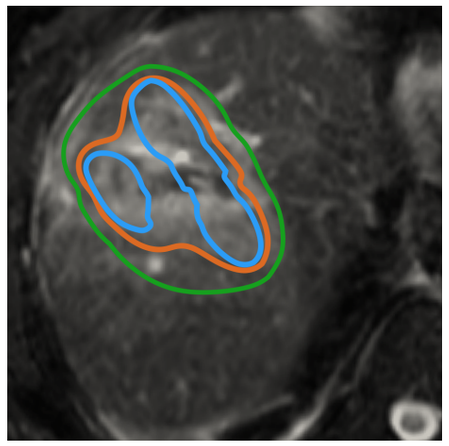

T2 w

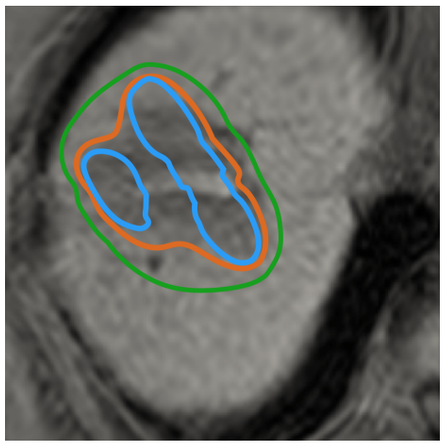

T1w

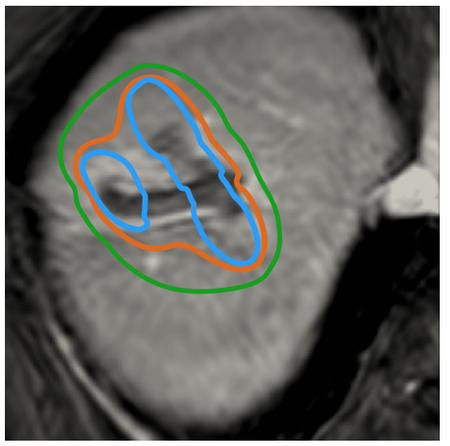

T1 injection

Irreversible zone for each of the 3 pullbacks

Necrosis (blue), irreversibly (orange) and reversibly permeabilised regions at the end of the procedure

Conclusions and perspectives

EP: a promising ablation technique, especially for liver and pancreatic cancers, but the threshold to generate cell death have to be determined precisely.

There is a need for more numerical investigations.

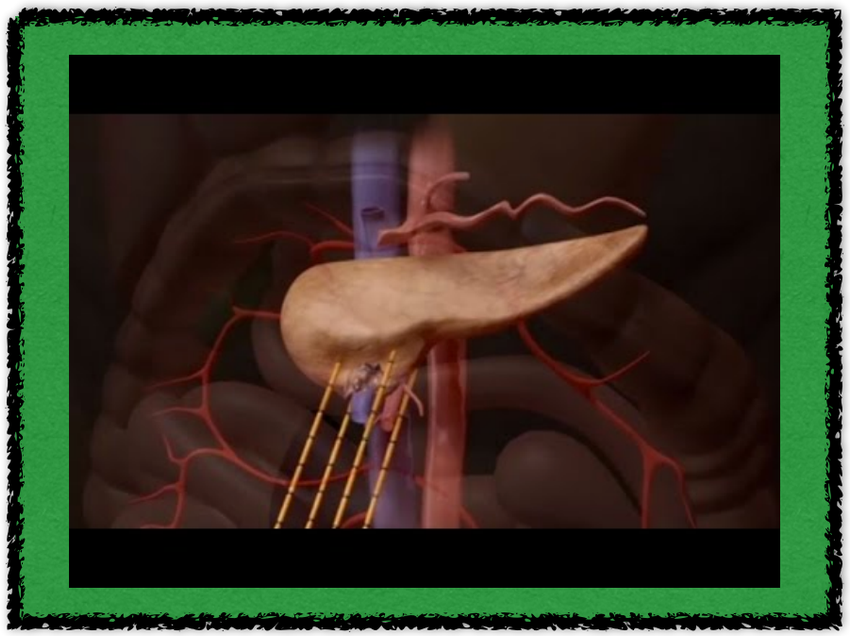

Immunogenicity of EP therapies

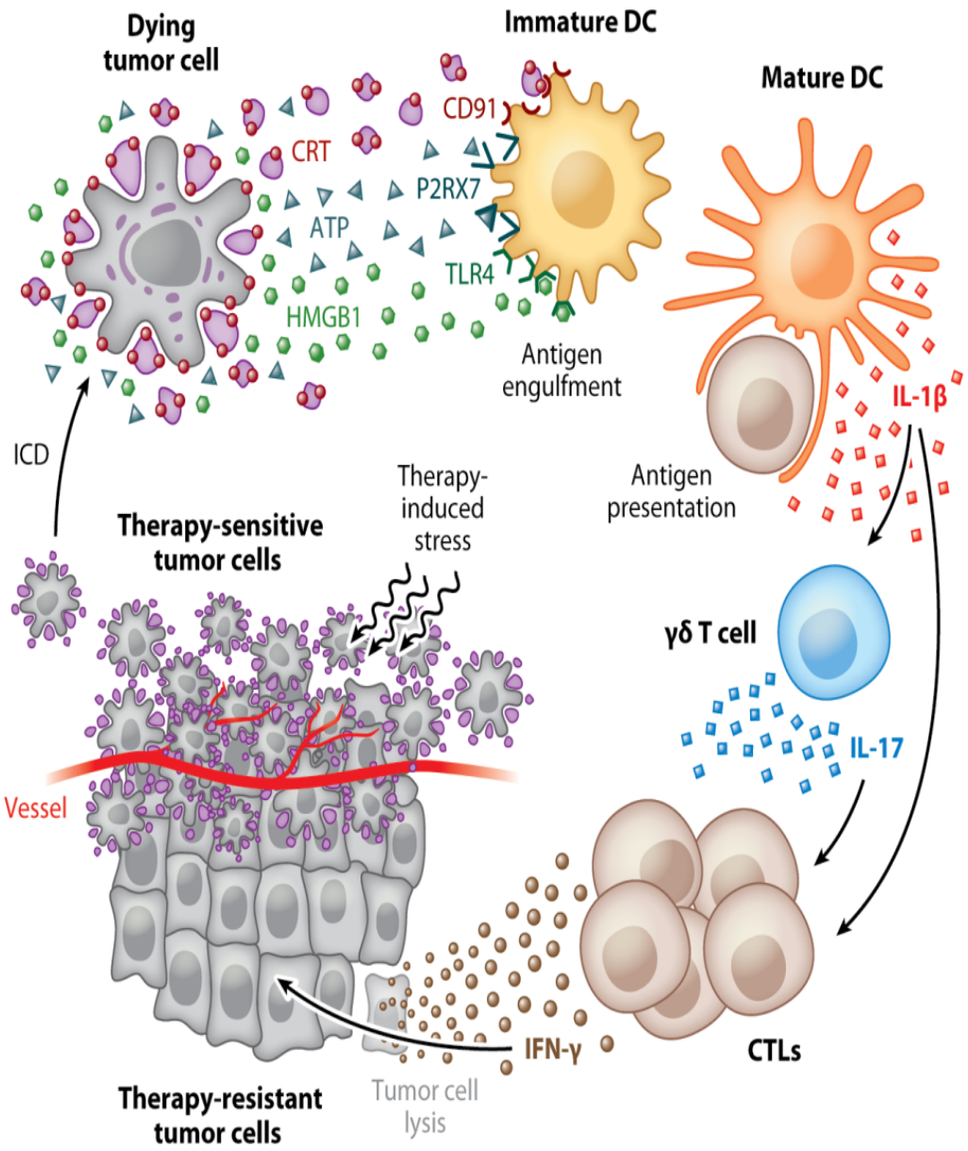

- **ATP release**: autophagy

« find me » signal for DCs : IL-1β production

➔ activation of IL-17+ **γδ T c**ells and CD8+ T cells

Favors DC differentiation and maturation

- **Exposure of Calreticuline (CRT)**:

Endoplasmic reticulum stress

« eat-me » signal for DCs

- **HMGB1 release**:

membrane disruption

Pro-inflammatory cytokine

Favors cross-presentation of tumor antigens by DCs

Immunogenicity of EP therapies

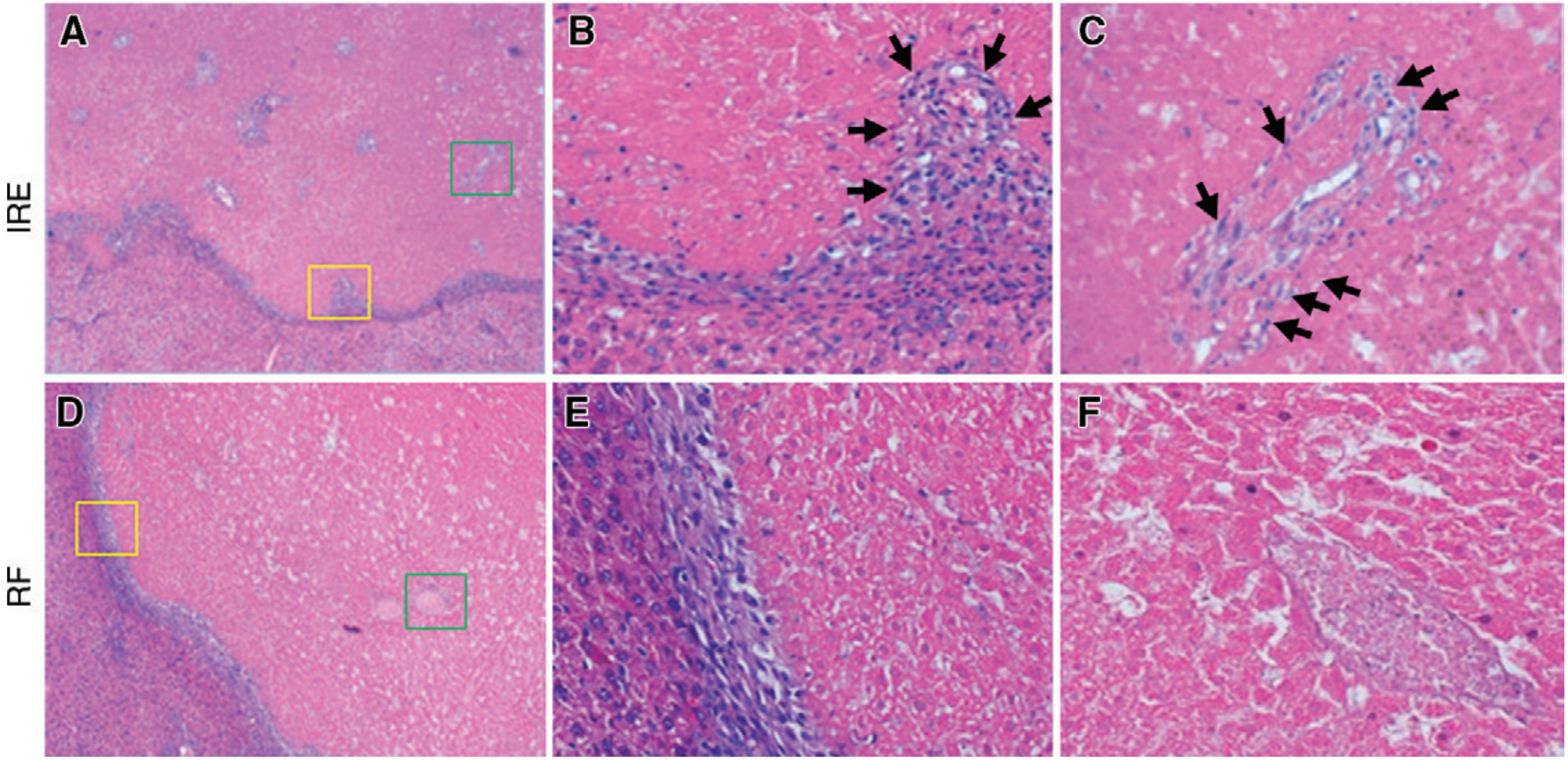

Acknowledgments

D. Voyer
EIGSI & MONC

Team MONC

O. Séror

J-P Tasu

O. Sutter

THANK YOU!

Some references

On EP modeling

M. Leguèbe, A. Silve, L.M. Mir, C. Poignard. "Conducting and Permeable States Membrane Submitted to High Voltage Pulses. Mathematical and Numerical Studies Validated by the Experiments". Jnl. Th. Biol. Vol. 360, (2014)

C. Poignard, A. Silve, L. Wegner. "Different Approaches used in Modeling of Cell Membrane Electroporation". in Handbook of Electroporation, Springer, 2018

T. Garcia-Sanchez, D. Voyer, C. Poignard, L.M. Mir. Physiological changes may dominate the electrical properties of liver during reversible electroporation: Measurements and modelling. Bioelectrochemistry, Vol. 136, (2020).

D.Voyer, A. Silve, L.M. Mir, R. Scorretti, C. Poignard. Dynamical modeling of tissue electroporation. Bioelectrochemistry, Vol. 119, (2018)

A.Collin, H. Bruhier, J. Kolosnjaj, M. Golzio, MP Rols, C. Poignard. Spatial mechanistic modeling for prediction of 3D multicellular spheroids behavior upon exposure to high intensity pulsed electric fields. AIMS Bioeng. (2022).

P. Jaramillo, A. Collin, C. Poignard. ``Phase-field model of bilipid membrane electroporation'' to appear in JoMB, (2023)

On EP ablation

L. Lafitte, R. Giraud, C. Zachiu, M. Ries, O. Sutter, A. Petit, O. Seror, C. Poignard, B. Denis de Senneville. Patch-based field-of-view matching in multi-modal images for electroporation-based ablations. Computerized Medical Imaging and Graphics, Vol. 84, (2020).

O. Séror, C. Poignard, O. Gallinato, R. Belkacem-Ourabia, O. Sutter. "Irreversible Electroporation: Disappearance of observable changes at imaging does not always imply complete reversibility of the underlying causal tissue changes". Letter published in Radiology, Vol. 282, Issue 1 (2017).

O. Gallinato, B. Denis de Senneville, O. Séror, C. Poignard. UNumerical Modelling Challenges for Clinical Electroporation Ablation Technique of Liver Tumors. Math. Model. Nat. Phenom., Vol. 15 (11), (2020).

O. Gallinato, B. Denis de Senneville, O. Séror, C. Poignard. Numerical workflow of irreversible electroporation for deep-seated tumor. Phys. Med. Biol., Vol. 64, (2019).

J. Tasu, M. Vionnet, S. Velasco, L. Lafitte, C. Poignard. Percutaneous irreversible electroporation for the treatment of pancreatic insulinoma. Letter in Diag, Interv. Imag. (2023)